CHIN. PHYS. LETT. Vol. 35, No. 6 (2018) 066801

Charge Density Wave States in 2H-$MoTe_2$ Revealed by Scanning Tunneling Microscopy *

Lu Dong(董璐)[1], Guan-Yong Wang(王观勇)[1], Zhen Zhu(朱朕)[1], Chen-Xiao Zhao(赵晨晓)[1], Xin-Yi Yang(杨心怡)[1], Ai-Min Li(李爱民)[1], Jing-Lei Chen(陈惊雷)[2], Dan-Dan Guan(管丹丹)[1,3], Yao-Yi Li(李耀义)[1,3], Hao Zheng(郑浩)[1,3], Mao-Hai Xie(谢茂海)[2], Jin-Feng Jia(贾金锋)[1,3]**

[1]*Key Laboratory of Artificial Structures and Quantum Control (Ministry of Education), School of Physics and Astronomy, Shanghai Jiao Tong University, Shanghai 200240*

[2]*Physics Department, The University of Hong Kong, Pokfulam Road, Hong Kong*

[3]*Collaborative Innovation Center of Advanced Microstructures, Nanjing 210093*

(Received 12 February 2018)

2H- and 1T′-phase monolayer $MoTe_2$ films on highly oriented pyrolytic graphite are studied using scanning tunneling microscopy and spectroscopy (STM/STS). The phase transition of $MoTe_2$ can be controlled by a post-growth annealing process, and the intermediate state during the phase transition is directly observed by STM. For 2H-$MoTe_2$, inversion domain boundaries are presented as bright lines at high sample bias, but as dark lines at lower sample bias. The dI/dV mappings reveal the distinct distributions of electronic states between domain boundaries and interiors of domains. It should be noted that a 2×2 periodic structure is clearly discernable inside the domains, where the STS measurement shows a small dip of size ∼150 meV at the vicinity of the Fermi level, indicating that the 2×2 periodic structure may be an incommensurate charge density wave. Moreover, a 4×4 periodic structure appears in 2H-$MoTe_2$ grown at a higher substrate temperature.

PACS: 68.37.Ef, 68.55.−a, 73.20.−r, 68.47.Fg DOI: 10.1088/0256-307X/35/6/066801

Compared with graphene, two-dimensional (2D) transition metal dichalcogenides (TMDCs) possess a strong spin orbit coupling.[1−4] They are attracting intensive research interests due to their intriguing electronic properties, such as charge density wave (CDW),[5−8] superconducting phase,[9−11] and 2D quantum spin Hall state.[12] TMDCs with the common formula MX_2 (where M = Mo, W, etc. and X = S, Se, Te) have different phases including the hexagonal (2H), octahedral (1T) and monoclinic or distorted octahedral (1T′) structures.[13−15] Different structures of the TMDCs have distinct electronic properties. For example, monolayer 1T′-MX_2 was theoretically predicted to be a 2D topological insulator with a large gap,[12] which was experimentally realized in the 1T′-WTe_2 lately.[16−18] The 2H-MX_2 draws attentions for its direct bandgaps in the visible spectrum range,[19−21] high charge carrier mobility[22,23] and potential applications in optoelectronic devices.[24−26] Recently, the monolayer 1T′- and 2H-$MoTe_2$ have been successfully fabricated by experiments,[27−29] but their surface structures and electronic properties, which are critical for exploring their new electrical and optical properties, remain scarcely studied.

The properties of 2D TMDCs can be modified by defects. Individual atomic-scale defects will tune the charge transport[30] or introduce ferromagnetism,[31] and one-dimensional defects such as domain boundaries or edges may drastically change their electronic and optical properties.[32,33] Domain boundaries in 2D TMDCs have been widely studied, e.g., the metallic states with a triangular configuration were observed at inversion domain boundaries (IDBs) of 2H-$MoSe_2$ by scanning tunneling microscopy and spectroscopy (STM/STS).[34] Recently, direct observation of the CDW, being located on the conducting mirror twin boundaries of monolayer $MoSe_2$ has been reported.[7] The CDW order is also observed in other 2D TMDCs such as 2H-$NbSe_2$[6,8] and 1T-TaS_2.[35,36] As for 2H-$MoTe_2$, we previously discovered similar triangular networks intertwined by domain boundaries like in 2H-$MoSe_2$,[27] but the electronic states of the domains boundaries and domains have not been studied in detail.

Here we report STM/STS studies of monolayer 2H- and 1T′-$MoTe_2$ grown on highly oriented pyrolytic graphite (HOPG) by molecular beam epitaxy (MBE). The phase transition of $MoTe_2$ is successfully tuned by a post-growth annealing process as reported in our previous work.[27] On the other hand, the intermediate state during the phase transition is directly revealed by STM. The topographic properties as well as electronic states of 2H-$MoTe_2$ are also carefully studied. Topographically, IDBs in 2H-$MoTe_2$ manifest as bright-line networks at high sample bias, but show as dark trenches at low sample bias. In addition, a 2×2 periodic structure is resolved inside the domains. However, IDBs are rarely observed on 2H-$MoTe_2$ samples grown at a higher substrate temperature. For the latter sample, a bias-dependent structural change from 2×2 to 4×4 is detected. Moreover, a small dip of size ∼150 meV is discerned near the Fermi level in

*Supported by the National Key Research and Development Program of China under Grant Nos 2016YFA0301003 and 2016YFA0300403, and the National Natural Science Foundation of China under Grant Nos 11521404, 11634009, U1632102, 11504230, 11674222, 11574202, 11674226, 11574201 and U1632272.

**Corresponding author. Email: jfjia@sjtu.edu.cn

© 2018 Chinese Physical Society and IOP Publishing Ltd

the STS taken within the 2×2 domain. Based on the above study, we attribute the 2×2 structure to the CDW.

Growth of monolayer $MoTe_2$ films was carried out in a customized Omicron MBE system with a base pressure better than 5×10^{-10} mbar. The HOPG substrate was degassed thoroughly in ultrahigh vacuum and flashed up to 600℃ prior to $MoTe_2$ deposition. Mo and Te were evaporated from an e-beam and a conventional Knudsen cell, respectively. During the $MoTe_2$ growth, the substrate was kept at a temperature ranging from 250℃ to 400℃. The film growth rate was about 0.3 monolayer/hour, which was determined by post-growth coverage measurement of the deposit by a room-temperature (RT) Omicron STM.[27] The samples were then capped by depositing an amorphous Te at RT before being taken out of vacuum for further studies in a separate Unisoku low-temperature STM. For the latter, after loaded into the Unisoku system, the samples were annealed at 250℃–300℃ to desorb the Te capping layer and then transferred to the STM stage for measurements at 77 K. The STM topographic images were taken at constant current mode using a tungsten tip. The dI/dV spectra were measured using a lock-in amplifier with a modulation voltage of 5 mV at 991 Hz.

Figure 1(a) shows a topographic image of the epitaxial $MoTe_2$ thin film grown on HOPG. The surface is partially covered by monolayer $MoTe_2$ islands. As shown in Fig. 1(b), the height of the monolayer $MoTe_2$ is slightly less than 1 nm. Figure 1(c) shows an atomically resolved STM image of 1T′-$MoTe_2$, which shows the typical stripe structures of the 1T′ phase. The lattice constants a and b are 0.620 nm and 0.335 nm, respectively, which are in agreement with the reported values.[27,29] The dI/dV spectrum of 1T′-$MoTe_2$ is shown in Fig. 1(d), which exhibits a typical semi-metallic feature. The 2H-$MoTe_2$ domains are also observed in the sample, where the bright domain boundaries with a triangular configuration are identified (Fig. 1(e)). The dI/dV spectrum of 2H-$MoTe_2$ reveals a ∼1.5 eV semiconducting gap (see Fig. 1(f)), which is larger than that in bulk.[37] Since the energy difference between 1T′ and 2H phases of $MoTe_2$ is small (∼43 meV per formula unit), the phase transition from 1T′ to 2H phase could be realized by increasing the temperature of post-growth annealing, as confirmed by our previous work.[27] Interestingly, an intermediate state during the phase transition is also captured by STM as shown in Fig. 1(g), where both triangular networks and the stripe structures are identified in the same region. The distance between two adjacent stripes is about 0.63 nm (see Fig. 1(h)), which matches well with 1T′-$MoTe_2$. To the best of our knowledge, this is the first experimental observation of the topography of intermediate state during the phase transition, providing very important information for understanding the kinetics and dynamics of phase transition from 1T′- to 2H-$MoTe_2$.

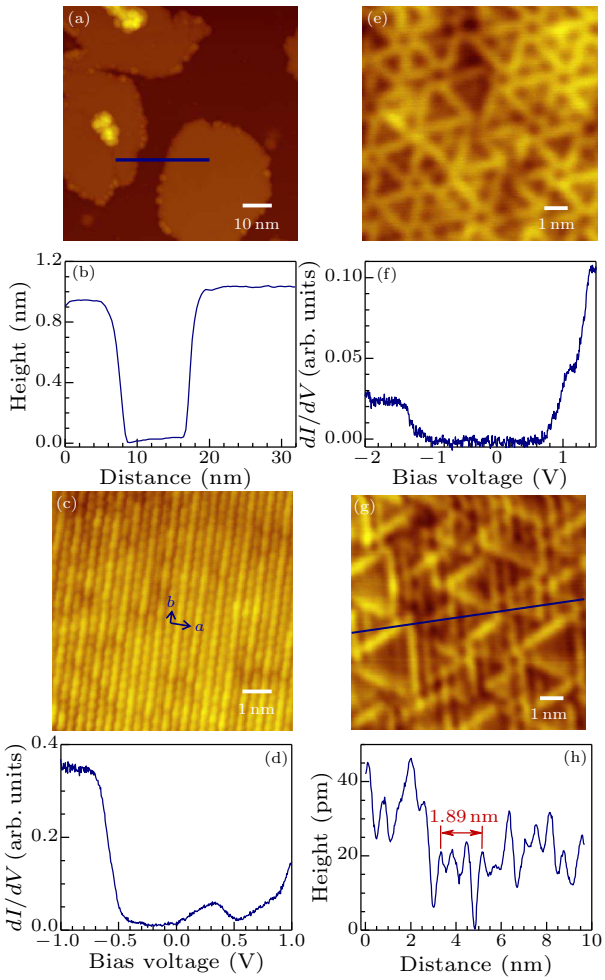

Fig. 1. STM images and dI/dV spectra of $MoTe_2$. (a) Large scale STM image of a $MoTe_2$ film, $V_s = 2.2$ V, and $I = 49$ pA. (b) Line profile along the blue line drawn in (a). (c) Atomically resolved STM image of 1T′-$MoTe_2$, $V_s = 26.6$ mV, and $I = 100$ pA. [(d), (f)] The dI/dV spectra measured on 1T′-$MoTe_2$ and 2H-$MoTe_2$, respectively. (e) STM image taken on 2H-$MoTe_2$, $V_s = 2$ V, and $I = 100$ pA. (g) STM image revealing the intermediate state of $MoTe_2$ during the phase transition, $V_s = 1.9$ V, and $I = 100$ pA. (h) Line profile along the blue line drawn in (g).

The electronic states of 2H-$MoTe_2$ are attentively probed. Figure 2(a) shows the topography of 2H-$MoTe_2$ at the sample bias of 1.9 V, where the bright triangular networks formed by IDBs can be clearly discerned. However, at a low sample bias, the domain boundaries appear as dark trenches (Fig. 2(b)), and a 2×2 periodic structure can be clearly resolved within the triangular domains. A more complex structure is also observed at a negative bias (see Fig. 2(c)). The variation of density of states depends strongly on bias, indicating that the STM contrast originates primarily from the modified electronic states rather than topographic features. However, previous works on 2H-$MoSe_2$ showed that the domain boundaries could be observed as bright lines only at negative sample bias.[7,34] This difference between 2H-$MoTe_2$ and 2H-$MoSe_2$ may reflect different effects caused by domain boundaries in these two different materials. Figure

2(d) displays dI/dV spectra obtained at a domain boundary and inside a domain, respectively. A comparison reveals apparent differences at both low and high sample biases, with a cross at ∼1.7 V. In addition, the dI/dV mappings also confirm the distinct distributions of electronic states between domain boundaries and the interiors of domains (see Figs. 2(e) and 2(f)). Recently, the different spatial distributions of the electronic states were also observed in 1T-TaS_2 and attributed to two distinct orbital textures.[38] These two different types of orbital textures were observed in Ref. [39] as well and used as the indicator of the CDW gap. Based on the above similarity between our findings in 2H-$MoTe_2$ and these reports, the 2×2 periodic structure could be attributed to CDW.

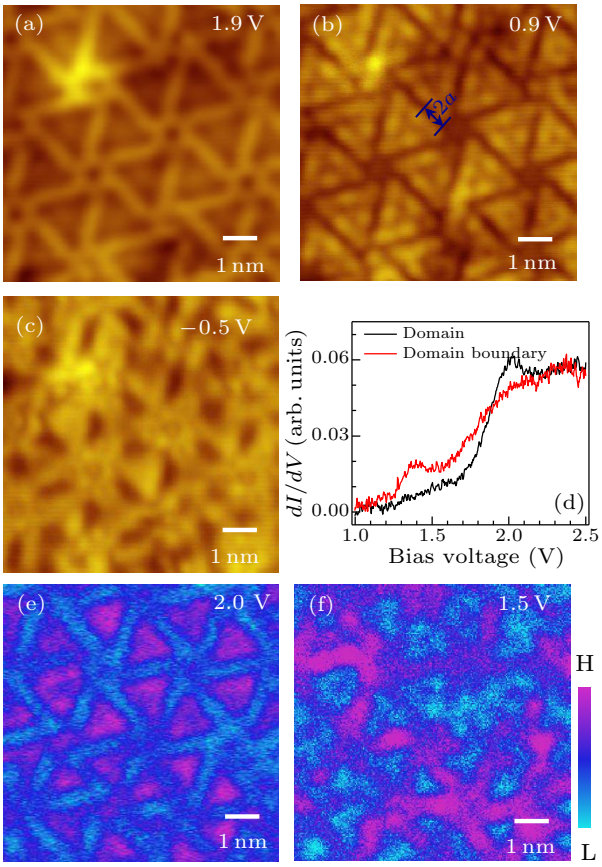

Fig. 2. Electronic states at domain boundaries and inside domains of 2H-$MoTe_2$. (a)–(c) Topography of 2H-$MoTe_2$ obtained at different biases with tunneling current $I = 100$ pA. (d) The dI/dV spectra of $MoTe_2$ taken at the domain boundary (red) and inside the domain (black). [(e), (f)] The dI/dV mappings at the biases of 2.0 V and 1.5 V, respectively.

It should be noted that topographic images of 2H-$MoTe_2$ are strongly dependent on the bias conditions as exemplified in Figs. 2(a)–2(c). A 2×2 periodic structure can be clearly resolved in Fig. 2(b), which is not originated from the Moiré patterns. The same bias-dependent 2×2 periodic structure is also observed in another sample grown at a higher substrate temperature (Figs. 3(a) and 3(b)). For the latter, there are no domain boundaries, resembling that of high-temperature grown 2H-$MoSe_2$ thin films.[40] In addition to the 2×2 structure, a 4×4 periodic structure is also resolved at a low sample bias of 0.1 V, of which the basic repeating unit is marked by a red parallelogram in Fig. 3(c). Figure 3(d) also displays the same 4×4 periodic structure but in another region of the sample. Fast Fourier transform (FFT) images of Figs. 3(a) and 3(c) are presented in Figs. 3(e) and 3(f), respectively. The 2×2 peaks are apparent in the FFT image (see Fig. 3(e)). It should be noted that in Fig. 3(f), not only 4×4 peaks but also weak 1×1 peaks are shown. However, the corresponding real space topographic image shown in Fig. 3(c) hardly reveals the 1×1 structure, which may be overwhelmed by the strong electronic states of 4×4 structure.

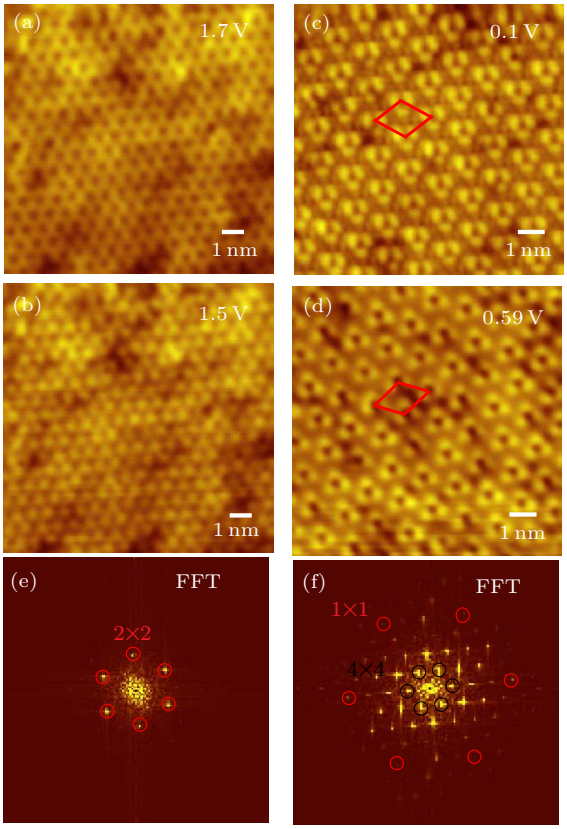

Fig. 3. STM images and the Fourier analysis of 2H-$MoTe_2$ film. (a)–(d) STM images of 2H-$MoTe_2$ film at different biases with tunneling current $I = 100$ pA. (a)–(c) are taken on the same area. The red parallelograms in (c) and (d) mark the unit cells. (e) The FFT of the STM image of (a). (f) The FFT of the STM image of (c).

For the 2×2 structure, we have performed detailed STS measurements aiming at realizing its origin and electronic characteristics. Figure 4(a) shows a topographic image of 2H-$MoTe_2$ at the sample bias of 2.0 V, at which the 2×2 periodicity no longer shows up. Figure 4(b) compares the dI/dV spectra measured at a domain boundary and inside a domain. As can be seen, a small dip of size ∼150 meV is observed in the vicinity of the Fermi level for the dI/dV spectrum taken inside a domain, whereas no such dip is observable at the domain boundary. A series of dI/dV spec-

tra taken along the line across the domain boundary are shown in Fig. 4(c). It is obvious that the dip only exists away from domain boundaries. This sharply contrasts with the case of 2H-$MoSe_2$, where a CDW gap was obtained only at the domain boundaries but not inside the domains. Hence, combining the incommensurate 2×2 periodic structure and the dip feature, there may be an incommensurate CDW (ICCDW) inside the domains of 2H-$MoTe_2$. The ICCDW state may be created by a simple phase shift of the commensurate CDW cross domains.

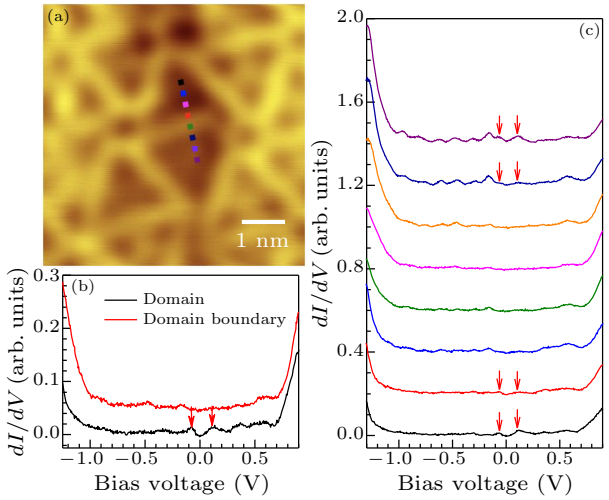

Fig. 4. The dI/dV spectra obtained at the domain boundary and inside the domain of 2H-$MoTe_2$. (a) STM image on a 2H-$MoTe_2$ thin film, $V_s = 2$ V, and $I = 100$ pA. (b) The dI/dV spectra taken on the 2H-$MoTe_2$ at a domain boundary (red) and inside a domain (black). (c) A series of dI/dV spectra measured along the dotted line across the domain boundary shown in (a). Spectra in (b) and (c) are shifted vertically for a clearer view.

In summary, monolayer $MoTe_2$ films grown on HOPG have been studied by STM/STS, where phase transition between 2H and 1T′ structures by a post-growth annealing process is confirmed. Importantly, an intermediate state is captured by STM, which can be of important information for understanding the phase transition kinetics and dynamics. For 2H-$MoTe_2$, dI/dV mappings reveal distinct distributions of electronic states between domain boundaries and the interiors of domains. In particular, a 2×2 periodic structure is resolved within domains and a 150 meV wide conductance dip in the STS spectra is observed near the Fermi level. These results suggest an ICCDW in 2H-$MoTe_2$. In addition, a 4×4 periodic structure is observed in 2H-$MoTe_2$ grown at a higher substrate temperature, though its origin is unclear and requires further investigations.

References

[1] Zhu Z Y, Cheng Y C and Schwingenschlögl U 2011 *Phys. Rev.* B **84** 153402
[2] Sun L, Yan J, Zhan D, Liu L, Hu H et al 2013 *Phys. Rev. Lett.* **111** 126801
[3] Manzeli S, Ovchinnikov D, Pasquier D, Yazyev OV and Kis A 2017 *Nat. Rev. Mater.* **2** 17033
[4] Zheng H, Bian G, Chang G, Lu H, Xu S Y et al 2016 *Phys. Rev. Lett.* **117** 266804
[5] Dai J, Calleja E, Alldredge J, Zhu X, Li L et al 2014 *Phys. Rev.* B **89** 165140
[6] Ugeda M M, Bradley A J, Zhang Y, Onishi S, Chen Y et al 2016 *Nat. Phys.* **12** 92
[7] Barja S, Wickenburg S, Liu Z F, Zhang Y, Ryu H et al 2016 *Nat. Phys.* **12** 751
[8] Yang H T, Tao H J and Zhao Z X 1998 *Chin. Phys. Lett.* **15** 123
[9] Qi Y, Naumov P G, Ali M N, Rajamathi C R, Schnelle W et al 2016 *Nat. Commun.* **7** 11038
[10] Pan X C, Chen X, Liu H, Feng Y, Wei Z et al 2015 *Nat. Commun.* **6** 7805
[11] Kang D, Zhou Y, Wei Y, Yang C, Guo J et al 2015 *Nat. Commun.* **6** 7804
[12] Qian X, Liu J, Fu L and Li J 2014 *Science* **346** 1344
[13] Wilson J A and Yoffe A D 1969 *Adv. Phys.* **18** 193
[14] Eda G, Fujita T, Yamaguchi H, Voiry D, Chen M and Chhowalla M 2012 *ACS Nano* **6** 7311
[15] Dawson W G and Bullett D W 1987 *J. Phys. C* **20** 6159
[16] Tang S, Zhang C, Wong D, Pedramrazi Z, Tsai H Z et al 2017 *Nat. Phys.* **13** 683
[17] Fei Z, Palomaki T, Wu S, Zhao W, Cai X et al 2017 *Nat. Phys.* **13** 677
[18] Wu S, Fatemi V, Gibson Q D, Watanabe K, Taniguchi T, Cava R J and Jarillo-Herrero P 2018 *Science* **359** 76
[19] Splendiani A, Sun L, Zhang Y, Li T, Kim J, Chim C Y, Galli G and Wang F 2010 *Nano Lett.* **10** 1271
[20] Zhang Y, Chang T R, Zhou B, Cui Y T, Yan H et al 2013 *Nat. Nanotechnol.* **9** 111
[21] Mak K F, Lee C, Hone J, Shan J and Heinz T F 2010 *Phys. Rev. Lett.* **105** 136805
[22] Baugher B W H, Churchill H O H, Yang Y and Jarillo-Herrero P 2013 *Nano Lett.* **13** 4212
[23] Kang K, Xie S, Huang L, Han Y, Huang P Y et al 2015 *Nature* **520** 656
[24] Geim A K and Grigorieva I V 2013 *Nature* **499** 419
[25] Lee C H, Lee G H, Zande AM van der, Chen W, Li Y et al 2014 *Nat. Nanotechnol.* **9** 676
[26] Kadir N A A, Ismail E I, Latiff A A, Ahmad H, Arof H and Harun S W 2017 *Chin. Phys. Lett.* **34** 014202
[27] Chen J, Wang G, Tang Y, Tian H, Xu J et al 2017 *ACS Nano* **11** 3282
[28] Naylor C H, Parkin W M, Ping J, Gao Z, Zhou Y R et al 2016 *Nano Lett.* **16** 4297
[29] Yu Y, Wang G, Qin S, Wu N, Wang Z, He K and Zhang X A 2017 *Carbon* **115** 526
[30] Qiu H, Xu T, Wang Z, Ren W, Nan H et al 2013 *Nat. Commun.* **4** 2642
[31] Cai L, He J, Liu Q, Yao T, Chen L et al 2015 *J. Am. Chem. Soc.* **137** 2622
[32] Bao W, Borys N J, Ko C, Suh J, Fan W et al 2015 *Nat. Commun.* **6** 7993
[33] Zande AM van der, Huang P Y, Chenet D A, Berkelbach T C, You Y M et al 2013 *Nat. Mater.* **12** 554
[34] Liu H, Jiao L, Yang F, Cai Y, Wu X et al 2014 *Phys. Rev. Lett.* **113** 066105
[35] Núñez-Regueiro M D, Lopez-Castillo J M and Ayache C 1985 *Phys. Rev. Lett.* **55** 1931
[36] Fu W, Chen Y, Lin J, Wang X, Zeng Q et al 2016 *Chem. Mater.* **28** 7613
[37] Böker T, Severin R, Müller A, Janowitz C, Manzke R et al 2001 *Phys. Rev.* B **64** 235305
[38] Qiao S, Li X, Wang N, Ruan W, Ye C et al 2017 *Phys. Rev. X* **7** 041054
[39] Cho D, Cho Y H, Cheong S W, Kim K S and Yeom H W 2015 *Phys. Rev.* B **92** 085132
[40] Jiao L, Liu H, Chen J, Yi Y, Chen W et al 2015 *New J. Phys.* **17** 053023